AD-A072 539 HUGHES RESEARCH LABS MALIBU CALIF F/G 20/5
OPTICAL-MICROWAVE INTERACTIONS IN SEMICONDUCTOR DEVICES.(U)
JUL 79 L FIGUEROA, C SLAYMAN, H W YEN N00173-78-C-0192
UNCLASSIFIED NL

| OF |
AD
A072539

END
DATE
FILMED
9-79
DDC

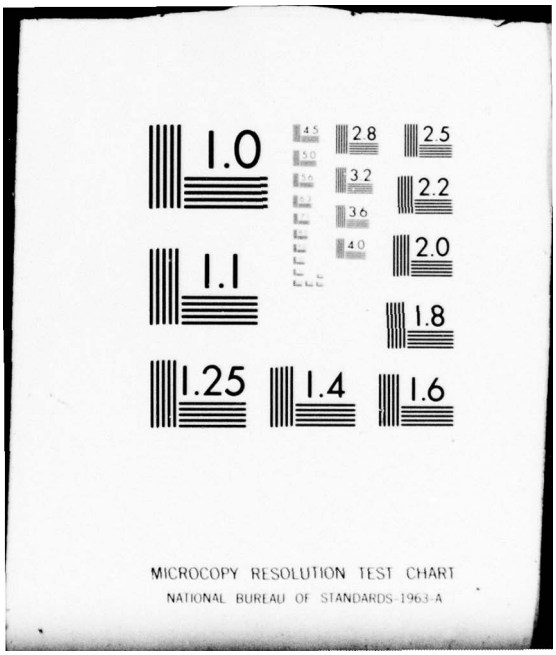
1.0
1.1
1.25
1.4
1.6
1.8
2.0
2.2
2.5
2.8
3.2
3.6
4.0
4.5
5.0
5.6
MICROCOPY RESOLUTION TEST CHART
NATIONAL BUREAU OF STANDARDS-1963-A

LEVEL II

P.S. 1

08

OPTICAL–MICROWAVE INTERACTIONS IN SEMICONDUCTOR DEVICES

L. Figueroa, C. Slayman and H. W. Yen
Hughes Research Laboratories
3011 Malibu Canyon Road
Malibu, CA 90265

July 1979

29p.

N00173–78–C–0192

Quarterly Report 4

For period 1 April 1979 through 30 June 1979

Approved for public release; distribution unlimited.

Quarterly rept. no. 4, 1 apr-30 Jun 79

Sponsored by
DEFENSE ADVANCED RESEARCH PROJECTS AGENCY
1400 Wilson Boulevard
Arlington, VA 22209

Prepared For
NAVAL RESEARCH LABORATORY
4555 Overlook Avenue, S.W.
Washington, DC 20375

172600

The views and conclusions contained in this document are those of the authors and should not be interpreted as necessarily representing the official policies, either expressed or implied, of the Defense Advanced Research Projects Agency or the U.S. Government.

UNCLASSIFIED

SECURITY CLASSIFICATION OF THIS PAGE (When Data Entered)

REPORT DOCUMENTATION PAGE		READ INSTRUCTIONS BEFORE COMPLETING FORM
1. REPORT NUMBER	2. GOVT ACCESSION NO.	3. RECIPIENT'S CATALOG NUMBER
4. TITLE (and Subtitle) OPTICAL-MICROWAVE INTERACTIONS IN SEMICONDUCTOR DEVICES A068387		5. TYPE OF REPORT & PERIOD COVERED Quarterly Report 4 1 April 1979-30 June 1979 6. PERFORMING ORG. REPORT NUMBER
7. AUTHOR(s) L. Figueroa, C. Slayman, and H.W. Yen		8. CONTRACT OR GRANT NUMBER(s) N00173-78-C-0192
9. PERFORMING ORGANIZATION NAME AND ADDRESS Hughes Research Laboratories 3011 Malibu Canyon Road Malibu, CA 90265		10. PROGRAM ELEMENT, PROJECT, TASK AREA & WORK UNIT NUMBERS
11. CONTROLLING OFFICE NAME AND ADDRESS Defense Advanced Research Projects Agency 1400 Wilson Boulevard Arlington, VA 22209		12. REPORT DATE July 1979 13. NUMBER OF PAGES 28
14. MONITORING AGENCY NAME & ADDRESS (if different from Controlling Office) Naval Research Laboratory 4555 Overlook Ave., S.W. Washington, DC 20375		15. SECURITY CLASS. (of this report) UNCLASSIFIED 15a. DECLASSIFICATION DOWNGRADING SCHEDULE

16. DISTRIBUTION STATEMENT (of this Report)

Approved for public release; distribution unlimited.

17. DISTRIBUTION STATEMENT (of the abstract entered in Block 20, if different from Report)

18. SUPPLEMENTARY NOTES

79 08 8 080

19. KEY WORDS (Continue on reverse side if necessary and identify by block number)

Mode-locking of injection lasers, optical fiber resonators, GaAs FETs, GaAs Gunn diodes, high-speed optical modulation, liquid phase epitaxial crystal growth

20. ABSTRACT (Continue on reverse side if necessary and identify by block number)

The study of injection-laser mode locking was continued. The lasers were operated in the external cavity configuration using a piece of optical fiber. Pumping injection lasers with short electrical pulses at a frequency corresponding to the round-trip transit frequency of the cavity generated stable optical pulses. A modified GaAs FET structure was designed such that efficient optical coupling to the active region of the device causes a strong optical-microwave interaction in the device for-

DD FORM 1 JAN 73 1473 EDITION OF 1 NOV 65 IS OBSOLETE

UNCLASSIFIED

SECURITY CLASSIFICATION OF THIS PAGE (When Data Entered)

high-speed optical detection, optical injection locking of oscillators, and optical-microwave mixing in amplifiers. Liquid phase epitaxial growth was used to grow the necessary GaAs and $Ga_{0.6}Al_{0.4}As$ layers on a semi-insulating substrate. Device fabrication is still in progress. Preliminary results showed that the devices exhibited a reasonable source-drain current versus source-drain voltage characteristic and are quite uniform over the entire wafer. A GaAs Gunn diode was designed and fabricated during the quarter. The diodes will be used to study the interaction between the injection laser's output and the high field Gunn domain in the diode. The ultimate goal is to achieve the efficient high-speed pulsed modulation of injection lasers. Diodes with various lengths were fabricated and tested using a curve tracer. Differential negative resistance was observed in all the diodes tested. Work on optical beam modulation using Gunn diodes is underway.

TABLE OF CONTENTS

Section		Page
	PREFACE	4
1	INTRODUCTION AND SUMMARY	5
2	RECENT RESULTS ON OPTICAL PULSE GENERATION USING INJECTION LASERS	7
3	DESIGN AND FABRICATION OF MODIFIED GaAs FETs	12
4	DESIGN AND FABRICATION OF GaAs GUNN DIODES FOR OPTICAL MODULATION	20
5	PLANS FOR THE NEXT QUARTER	27
	REFERENCES	28

PREFACE

The following personnel contributed to the research work reported here: L. Figueroa, C. Slayman, H.W. Yen, M.K. Barnoski, A. Yariv (consultant), and D.F. Lewis.

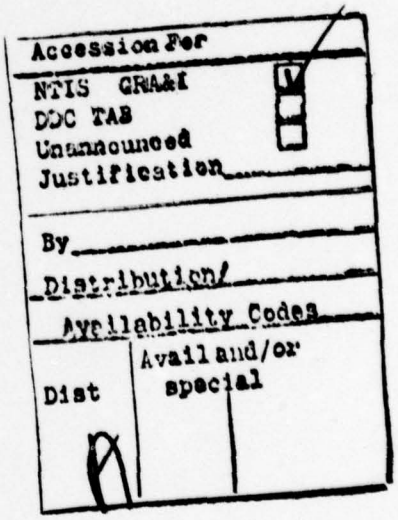

SECTION 1

INTRODUCTION AND SUMMARY

The goal of this research program is to develop unique hybrid optical-microwave semiconductor devices with optimal optical-microwave interaction characteristics for selected system applications and to investigate various methods of achieving the efficient high-frequency modulation of semiconductor lasers.

The study of injection laser mode locking was continued during this quarter (the fourth). We operated the laser in the external-cavity configuration using a piece of optical fiber. Pumping injection lasers with short electrical pulses at a frequency corresponding to the round-trip transit frequency of the cavity generated stable optical pulses. An autocorrelation measurement system for determining the width of the optical pulse was designed and is currently being assembled.

The major effort of the quarter was to develop a specialized GaAs FET device and a GaAs Gunn diode. The specialized FET was designed so that efficient optical coupling to the active region of the device will cause a strong optical-microwave interaction in the device for optical detection, optical injection locking, and optical mixing purposes. Liquid phase epitaxial (LPE) growth was used to grow the necessary GaAs and $Ga_{0.6}Al_{0.4}As$ layers on a semi-insulating GaAs substrate. Layers were characterized to ensure good quality. A set of four masks was needed to fabricate the special FETs. The masks have been designed and procured, and the FETs are currently being fabricated. Preliminary results showed that the devices exhibited reasonable characteristics and that their properties were quite uniform over the entire wafer.

GaAs Gunn diodes are also being fabricated. These diodes will be used to study the interaction between the output of an injection laser and the high-field Gunn domain in the diode. The ultimate goal is to achieve efficient high-speed modulation of the injection laser output.

The Gunn diodes were fabricated on a two-layer structure that was quite similar to the one used for the FETs with the exceptions that layer thickness and doping concentration were different. Several devices were fabricated and tested using a curve tracer. Differential negative resistance was observed in all the diodes tested. Work on optical beam modulation using Gunn diodes will be carried out next quarter.

SECTION 2

RECENT RESULTS ON OPTICAL PULSE GENERATION USING INJECTION LASERS

In the last quarterly report, we described an extensive experimental study of mode locking in semiconductor lasers with two different external-cavity configurations. In the first case, a spherical mirror was used in conjunction with the laser to form an ∿5-cm-long external cavity. Laser pulses less than 200 psec wide at an ∿3-GHz repetition rate were generated by modulating the laser current sinusoidally at the same frequency. In the second case, a piece of graded-index multimode fiber was used to replace the spherical mirror resonator. This allowed the cavity length to be varied quite easily and also simplified the alignment process. We were able to modulate the laser output at frequencies up to 4.26 GHz efficiently with the lasers biased only slightly above threshold.

During this quarter, we continued the experiment with the optical fiber resonator configuration (case two above). To ease the problem of fiber alignment, we improved the fiber fixture by using a piece of silicon wafer. An array of parallel V grooves separated by ∿250 μm were formed on the wafer using the preferential etching technique. We were able to mount several fibers with different lengths on one wafer. That the fibers were parallel was ensured by the etched V grooves: when one of the fibers was aligned to the laser, a simple translation of the silicon wafer could bring the rest of the fibers very close to perfect alignment. This feature allows the length of the external cavity of the injection laser to be varied easily by moving from one fiber to another.

In our previous experiments on the active mode locking of injection lasers, the perturbation necessary to induce longitudinal mode coupling was provided by a sinusoidal modulation of the laser current. We recently began experimenting with a different type of perturbation.

This was done by driving the lasers with short electrical pulses at the cavity round-trip transit frequency. The technique of using short-pulse excitation to mode lock a laser has been used successfully with dye lasers, where a mode-locked Ar^+ laser pulse train was used to synchronously excite the dye and thus produce ultrashort dye laser pulses. In our experiment, we used short electrical pulses to excite the injection laser and generate short optical pulses at an ∿1-GHz repetition rate. The short electrical pulses were generated by a step-recovery diode with a 1-GHz center frequency and a useful band of ±100 MHz. The diode can provide useful harmonic power up to 18 GHz when driven by a 1-GHz sinusoidal signal. Therefore, it should be very efficient for mode locking an injection laser. Unfortunately, the laser package and the circuit around the laser do not have the bandwidth to accommodate the sharp electrical pulse and hence the effectiveness of this scheme is limited unless a broadband circuit is used.

The experimental arrangement is essentially the same as that described in the last report with slight modifications, as shown in Figure 1. The step-recovery diode was placed in series with the rf input port of the laser driving circuit. Figure 2 shows a temporal display of the laser output power. The fiber external resonator of the laser was ∿9.3 cm long, corresponding to a round-trip transit frequency of ∿1.1 GHz. Figure 2(a) shows the case when the fiber was not properly aligned to the laser; optical output resembles that of a simple sinusoidal modulation. Figure 2(b) shows the case when the fiber was well aligned to the laser; considerable sharpening of the output was observed. The pulse width displayed was detector limited, indicating a pulse width of less than 150 psec. In both cases, the rf input power and the dc bias to the laser were roughly the same. We also noticed that the pulses produced by this technique were less noisy than those generated with sinusoidal current modulation.

The laser cavity resonance can, interestingly enough, be excited through an optical-electrical feedback loop. For example, when the

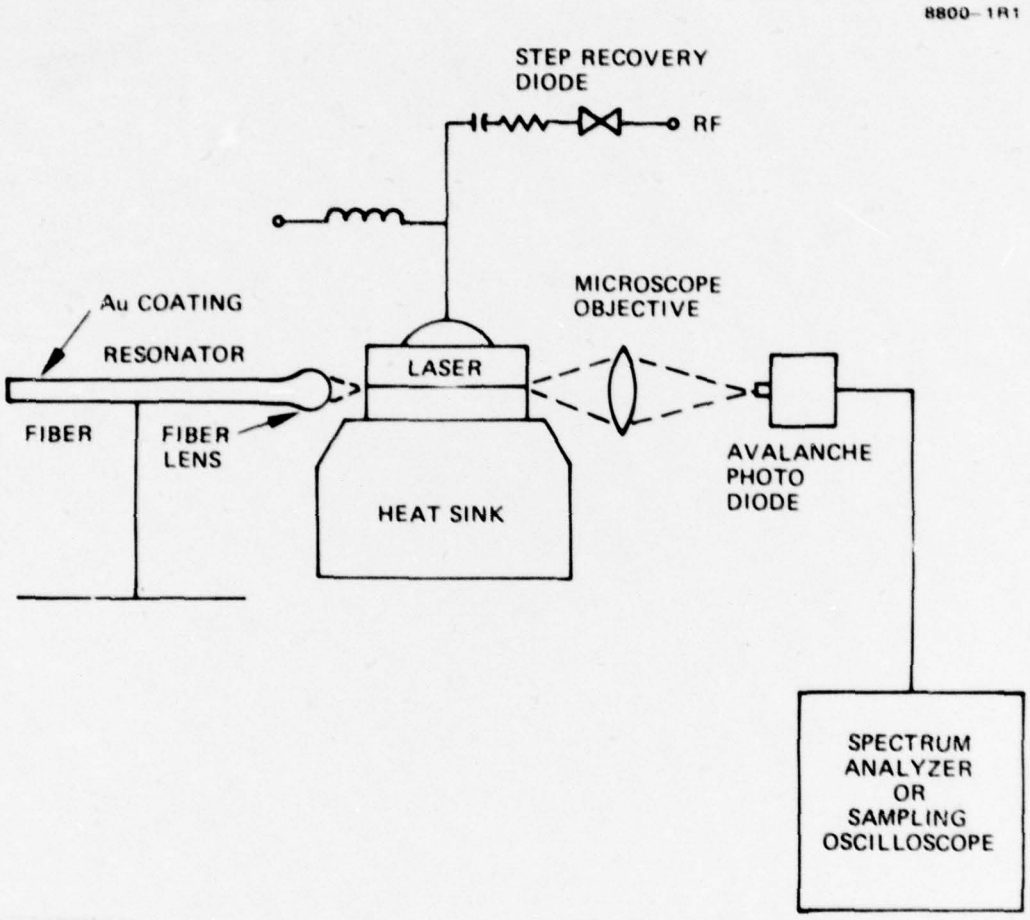

Figure 1. Experimental arrangement of injection-laser mode-locking study.

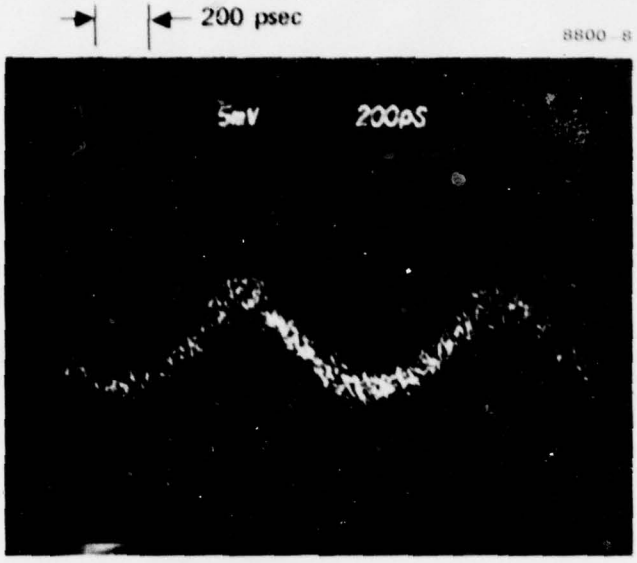

(a) No alignment.

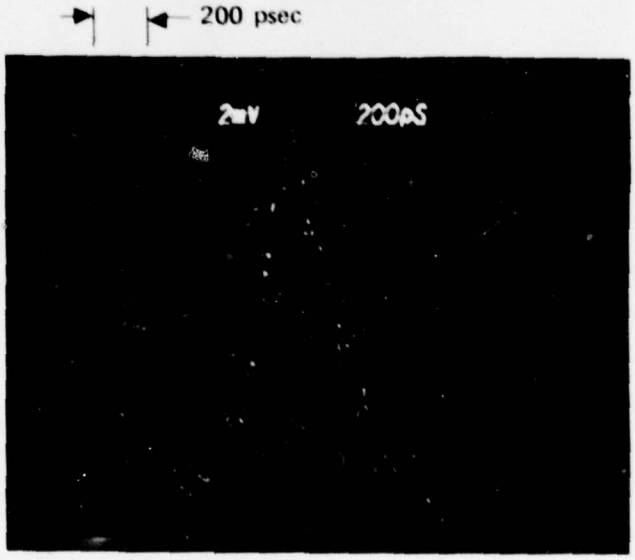

(b) With alignment.

Figure 8. Temporal display of synchronously pumped injection laser output.

laser is aligned to an external resonator, the output detected by a photodiode and displayed on the microwave spectrum analyzer will always show a resonance corresponding to the round-trip transit frequency of the cavity. If the photodiode output is amplified and fed back to the rf input port of the laser circuit, the spectrum analyzer will show enhanced resonance peaks corresponding to those frequencies with correct phase shift for positive feedback. These microwave resonance peaks can spread over a range of a few hundred megahertz if the feedback circuit used is relatively wideband. We also inserted a line stretcher in the feedback loop and observed the changes in the relative height of these peaks by varying the electrical length of the feedback path. This technique might be an important way of turning laser noise (self-pulsation) to advantage by changing it into stable and useful modulated laser output.

An autocorrelation measurement system using phase-matched second-harmonic generation is currently being assembled for recording the true optical pulse width. The nonlinear medium to be used is a piece of $LiIO_3$ crystal. The incident angle for phase-matched second-harmonic generation in this crystal at 8400 Å was calculated to be $\sim 38°$ with respect to the crystal axis. We have obtained and polished a piece of $LiIO_3$ crystal. Optical components such as a motor-driven precision translation stage, beam splitters, mirrors, and a rotation stage are being procured. Future work with laser mode locking will be to obtain higher repetition frequencies and shorter pulse widths and to study the phase jitter in optical pulses.

SECTION 3

DESIGN AND FABRICATION OF MODIFIED GaAs FETs

To achieve efficient optical injection locking, mixing, and high-speed detection using GaAs FET amplifiers or oscillators, we are interested in improving the coupling efficiency of light into GaAs FETs. A modified FET structure was proposed and analyzed in our last quarterly report. This device has a Burrus-type structure, as shown in Figure 3. The material preparation for the device is to start with a piece of Cr-doped GaAs semi-insulating substrate and to grow successively an n-$Ga_{1-x}Al_xAs$ ($\sim$5-μm-thick) layer and an n-GaAs ($\sim$1-μm-thick) layer. The GaAs layer is the active region of the FET and the $Ga_{1-x}Al_xAs$ layer acts as a buffer layer. For this device to work properly, there must be no current leaking through the $Ga_{1-x}Al_xAs$ layer. This can be done by leaving the $Ga_{1-x}Al_xAs$ layer undoped so as to keep its conductivity low and by choosing an appropriate percentage of Al such that the $Ga_{1-x}Al_xAs$ layer becomes an indirect bandgap material to further reduce the carrier mobility. Furthermore, since the bandgap energy of $Ga_{1-x}Al_xAs$ is higher than that of GaAs, the heterojunction also serves to confine charge carriers in the GaAs layer. Thus, the current leakage due to the presence of the $Ga_{1-x}Al_xAs$ layer can be kept at a minimum.

LPE crystal growth and layer characterization are very important for this task. The layers were grown with the conventional horizontal-boat, sliding-bar technique and characterized using a four-point probe and Hall-effect measurement setup. Data measured for several $Ga_{1-x}Al_xAs$ and GaAs layers are summarized in Tables 1 and 2. Table 1 gives the carrier concentration, mobility, resistivity, and sheet resistance for four different samples. It is clear from the table that the carrier mobility drops significantly as the material turns into indirect-gap ($x > 0.37$) material. Also, it appears that, by using high-purity single-crystal source material, $Ga_{0.6}Al_{0.4}As$ layers with resistivities

8567-3a

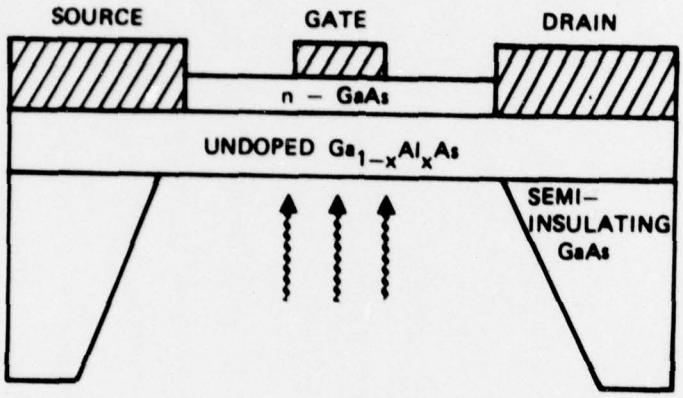

Figure 3. Modified GaAs FET structure with back-illumination access.

Table 1. Characteristics of LPE-Grown $Ga_{1-x}Al_xAs$ Layers (∿5 μm)

	ALUMINUM CONTENT x	CARRIER CONCENTRATION N (CM^{-3})	CARRIER MOBILITY μ ($CM^2/V \cdot SEC$)	RESISTIVITY ρ (Ω – CM)	SHEET RESISTANCE R_s (Ω)
GROWN WITH HIGH PURITY SOURCE	0.4	6.13×10^{15}	100	10.15	2.03×10^4
	0.25	3.83×10^{15}	1427	1.14	2.28×10^3
GROWN WITH POLY-CRYSTALLINE SOURCE	0.4	1.18×10^{16}	148	3.57	7.15×10^3
	0.35	3.37×10^{15}	796	2.33	4.65×10^3

Table 2. Characteristics of LPE Grown GaAs Layers (∿1 μm)

NO.	CARRIER CONCENTRATION N (CM^{-3})	CARRIER MOBILITY μ($CM^2/V \cdot SEC$)	RESISTIVITY ρ (Ω –CM)	SHEET RESISTANCE R_s (Ω)
1	2.23×10^{17}	2913	9.60×10^{-3}	96.0
2	7.76×10^{16}	2925	2.74×10^{-2}	274.0
3	1.19×10^{17}	3573	1.46×10^{-2}	146.5
4	7.12×10^{16}	3335	2.62×10^{-2}	262.0

higher than 10 Ωcm can be grown. Table 2 gives data for a few n-GaAs layers doped with Sn. The doping concentration varies between 7×10^{16} and $2 \times 10^{17}/cm^3$. Excellent mobility and resistivity were obtained for our device requirement. Since all the $Ga_{0.6}Al_{0.4}As$ layers were not intentionally doped during growth, the measured doping concentrations of $3 \times 10^{15}/cm^3$ represent the background level of our epi-system.

To fabricate the device shown in Figure 3 will require a set of four masks. Schematics of the masks are shown in Figure 4. The first mask is used to define a GaAs active mesa so that current leakage around the gate in the GaAs layer is minimized. The second mask defines the source and drain electrodes using the lift-off technique. The third mask defines the gate electrode, also by the lift-off technique, and the fourth mask is for etching the back side of the FET to open the illumination window. Various registration marks are put onto the masks to ensure proper alignment throughout the processing steps.

During the last quarter, we processed several wafers using the following procedure. After the layers were grown, the wafers were cleaned and coated with Shipley AZ1350J photoresist. The first mask was then used to define the active mesa pattern. This was followed by chemically etching the mesa pattern into GaAs. The etchant used was Superoxol (H_2O_2:NH_4OH). The etching rate of this process depends strongly on the pH value of Superoxol. A few measured values for n-GaAs are listed below:

pH	Etch Rate, μm/min
8.0	2
8.5	5
9.0	8 to 10

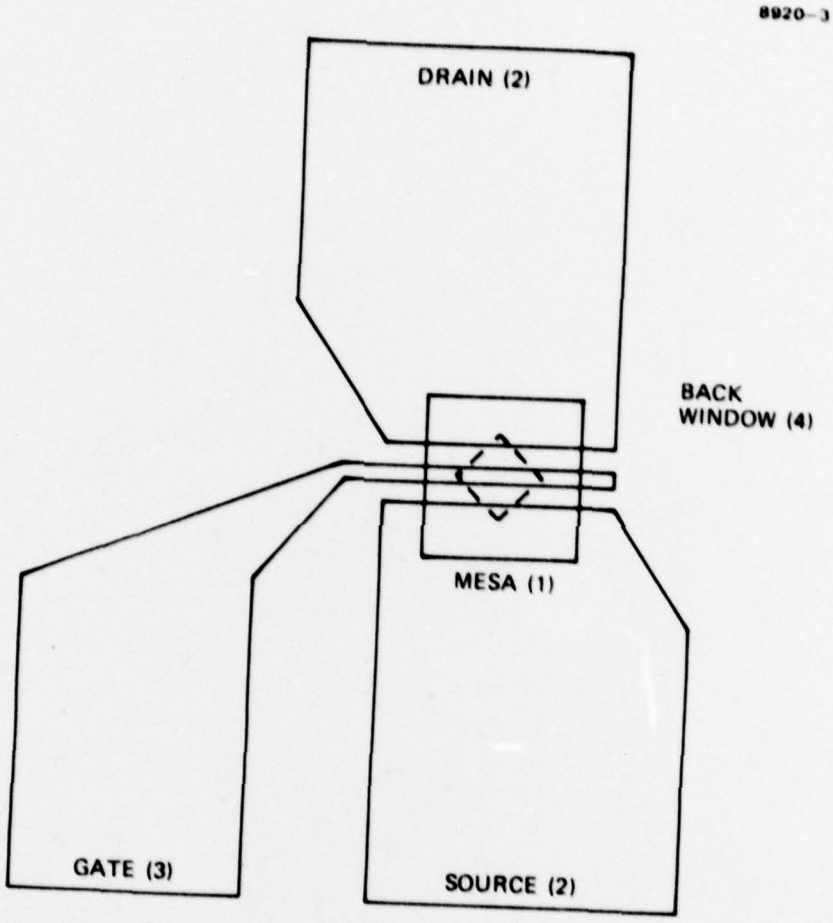

Figure 4. GaAs FET mask patterns. The numbers indicate the processing sequence.

Since Superoxol is a selective etchant, the process stops at the $Ga_{0.6}Al_{0.4}As$ surface and a GaAs mesa is formed. A second photoresist coating is then applied to the wafer and exposed to generate the source and drain electrode patterns. The electrodes are laid down by depositing thin layers of Au:Ge, Ni, and Au onto the wafer. After removing the photoresist, the sample was heated at 450°C under hydrogen atmosphere for 45 sec to form Ohmic contacts at the source and the drain. At this point, the devices are examined for their I-V characteristics using a probe station and a curve tracer. A typical curve from our devices is shown in Figure 5. The saturation voltage of the devices without gate electrode is ∿6 V, and the saturation current is ∿25 mA. We have found the characteristics of devices from the same wafer to be quite uniform. To put the gate electrode on the device by the lift-off technique requires another photolithography step. The lift-off technique requires that the photoresist pattern have sharp edges. Considerable effort was put into determining the optimal time and temperature for photoresist exposure, development, and post-baking. Figure 6(a) shows the photoresist pattern of the gate electrode. Note the sharpness of the walls. Figure 6(b) gives a close-up of one of the corners. The gate electrode is formed by evaporating Al to form a Schottky barrier. In the next quarter we will perform rf characterization of the completed GaAs FETs and will etch illumination windows into the back side of the devices. The optical-microwave interaction efficiency will also be determined.

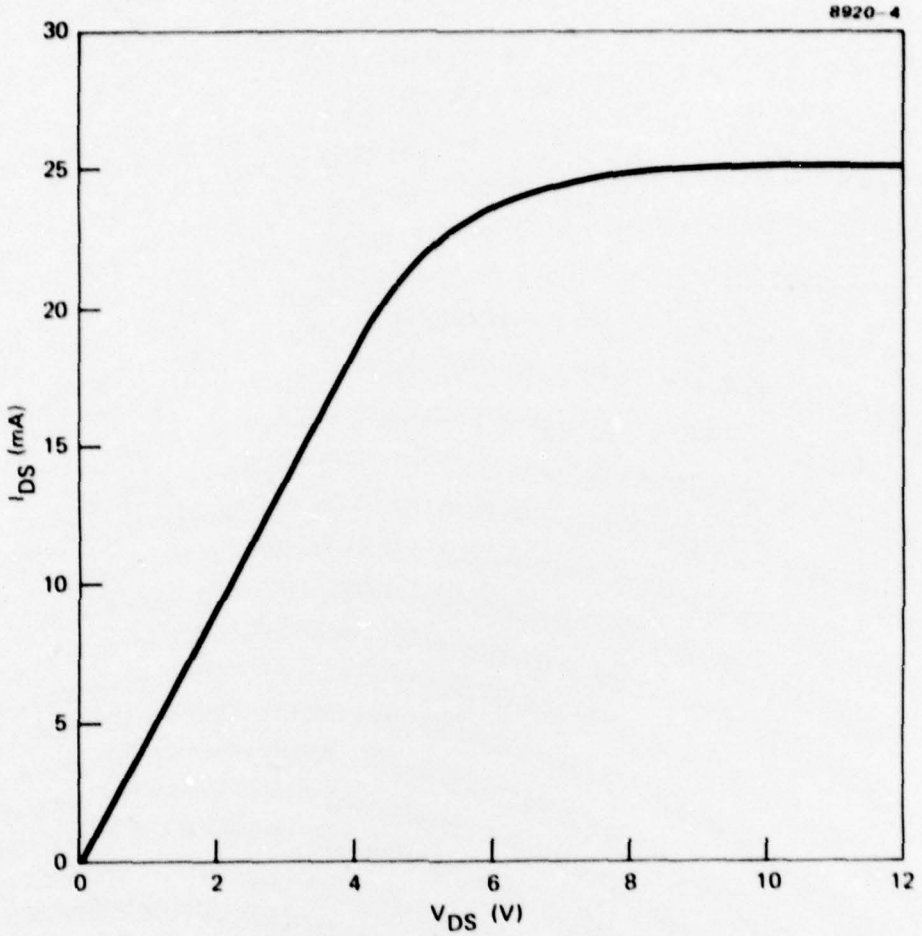

Figure 5. I-V curve of a GaAs FET without gate electrode.

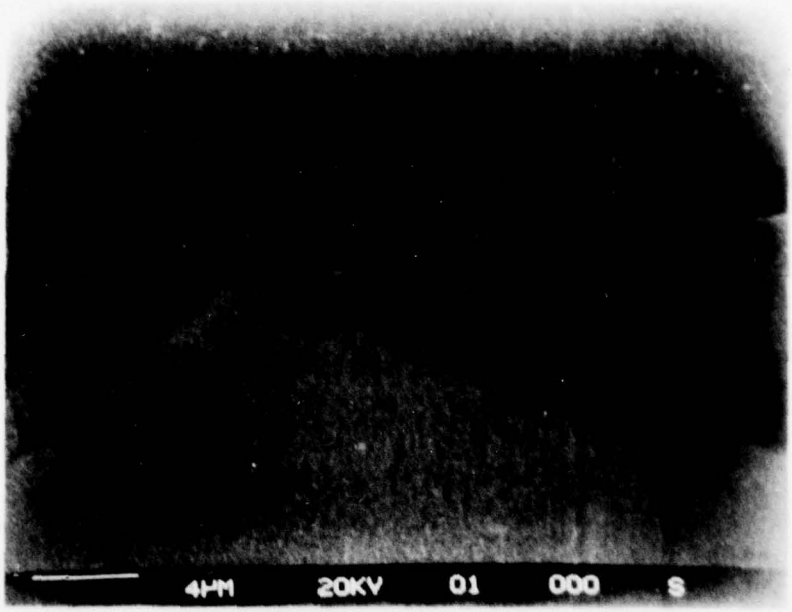

(a) Low magnification.

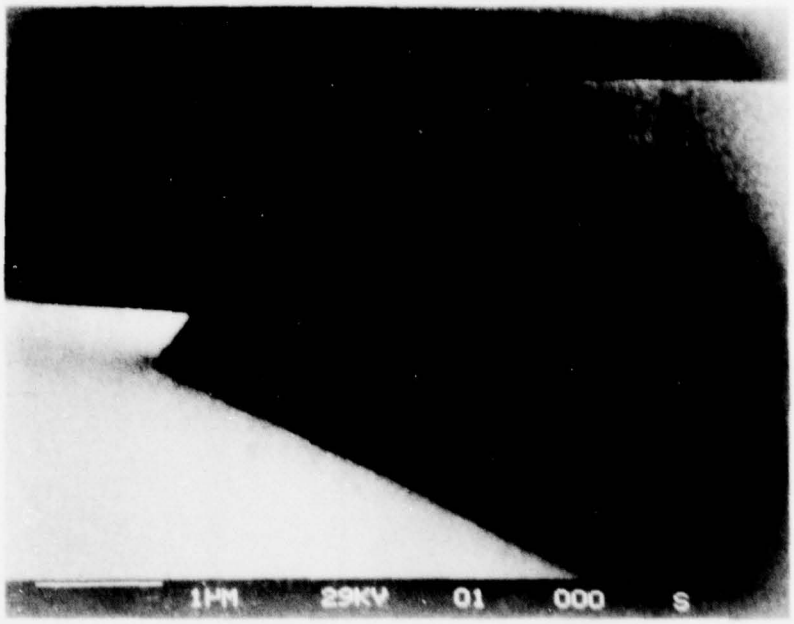

(b) Close-up of the inner corner.

Figure 6. Photoresist pattern of the gate electrode and bonding pad.

SECTION 4

DESIGN AND FABRICATION OF GaAs GUNN DIODES FOR OPTICAL MODULATION

The most common, and the easiest, method of modulating an injection laser is by varying the current that goes through the laser. However, this type of modulation is limited as to highest achievable modulation frequency because of the presence of the relaxation oscillation in the laser. State-of-the-art semiconductor lasers can be modulated efficiently up to only a few gigahertz with this method. A second drawback with direct modulation is that the laser, even though it oscillates at a single longitudinal mode under dc excitation, tends to break into multi-longitudinal mode oscillation when its current is modulated. Therefore, for ultrahigh frequency modulation, external modulators might be necessary.

This section describes a scheme in which the interaction between the traveling high electric field Gunn domain and the laser beam is used to achieve loss modulation of the laser output at very high frequencies.[1-3] The modulation frequency is determined by the operating frequency of the Gunn diode and is not limited by the frequency response of the laser. Thus, this is a promising method for the efficient high-frequency modulation of injection lasers and one that can possibly also be used for the active mode locking of injection lasers.

When a dc voltage is applied across a Gunn diode, high electric-field domains are formed in the device under certain conditions. These domains propagate between the two electrodes of a Gunn diode at a saturated velocity of $V_D \sim 10^7$ cm/sec. The traveling domains lead to a regular spiking of the device current at a frequency given by

$$f = V_d/L \ , \qquad (1)$$

where L is the length of the Gunn diode.

We propose to use the interaction between the Gunn domain and the optical beam to pulse modulate a semiconductor laser or LED at very high frequencies. Some of the important optical processes inside the Gunn domain are discussed below. The carrier density within a Gunn domain is higher than the background doping density. For a background doping concentration of $10^{16}/cm^3$, the peak carrier density is approximately 10 to 20 times that of the background. Thus the optical absorption due to free carriers is higher within the domain. A simple calculation reveals that the increase in absorption coefficient is on the order of 10 cm^{-1}. A second effect of the increased carrier density within the domain is that the real part of the dielectric constant will change. This leads to an increase in the optical reflectivity from the domain. However, since the change in the index of refraction Δn is only about 10^{-4}, the effect is negligible. We believe that the largest effect will come from the high electric fields within the domain. Since, by the well-known Franz-Keldysh effect, a large electric field can shift the absorption edge of a semiconductor (such as GaAs) to lower energies, the absorption coefficient will increase for an optical beam with given wavelength near the bandgap of the material. To estimate the change in absorption, we calculate the maximum electric field inside the domain using the expression[4]

$$E_{max} = \left(\frac{2eV_c n_o}{\varepsilon}\right)^{1/2} , \qquad (2)$$

where e is the electronic charge, V_c is the critical voltage, n_o is the carrier density, and ε is the dielectric constant of GaAs. The critical field $E_c = (V_c/L)$ in GaAs is $\sim 3 \times 10^3$ V/cm. For a 10-μm-long device, V_c is therefore ~3 V. Assuming a background doping concentration $n_o \cong 10^{16}/cm^3$, Eq. 2 yields $E_{max} \cong 10^5$ V/cm. The Franz-Keldysh effect is significant in the presence of such a strong electric field. Using available data for GaAs, we find that the change in absorption

coefficient, $\Delta\alpha$, can be as large as 500 cm^{-1} near the bandgap with a field of 10^5 V/cm. This large change can thus be used to pulse modulate the output from a GaAs injection laser (or LED).

The experimental arrangement to be used is shown in Figure 7. A Gunn diode is placed perpendicular to the injection laser cavity such that the laser output will go through the Gunn diode. The laser will be driven continuously, and the Gunn diode will be biased above the threshold for domain formation. The domains travel between the anode and the cathode at a frequency determined by Eq. 1. When the optical beam encounters a domain, the strong absorption of this region reduces the transmitted power, and when the domain disappears, the transmission is high. If we assume that the absorption coefficient is 500 cm^{-1} within the domain and 10 cm^{-1} outside the domain, then the extinction ratio I_{on}/I_{off} is given by

$$\frac{I_{on}}{I_{off}} = \frac{\exp(-10d)}{\exp(-500d)} = \exp(490d) ,$$

where d is the transverse dimension of the Gunn diode (the interaction length) expressed in centimeters. The list of extinction ratios versus d's shown in Table 3 indicates that efficient pulse modulation can be achieved with reasonable interaction distance. To enhance the interaction between the optical beam and the Gunn domain, we propose to use a waveguiding structure in the vertical direction, as shown in Figure 8. The Gunn diode is composed of two epitaxial layers, GaAs ($\sim$2 μm) and $Ga_{0.6}Al_{0.4}As$ ($\sim$2 μm) on a semi-insulating GaAs substrate. The doping level for the active GaAs layer is $\sim 10^{16}/cm^3$. The mask for the active region was designed and procured during this quarter. To achieve stable dc operation, we use a trapezoidally shaped active region with optimized geometrical parameters,[5] as shown in Figure 9(a). An etched pattern in GaAs is shown in Figure 9(b). We have fabricated

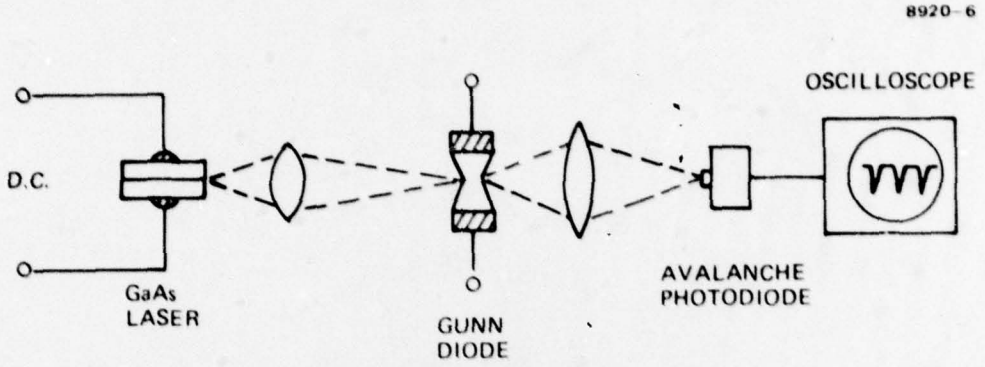

Figure 7. Experimental setup to be used for studying Gunn diode modulators.

Table 3. Extinction Ratio Versus Interaction Length of a Gunn Modulator

INTERACTION LENGTH d / EXTINCTION RATIO	I_{ON} / I_{OFF}		
20 (μm)	2.7	OR	4.31 dB
50	11.6		10.64 dB
70	30.8		14.89 dB
100	134.3		21.28 dB
150	1556.0		31.92 dB
200	18033.0		42.56 dB

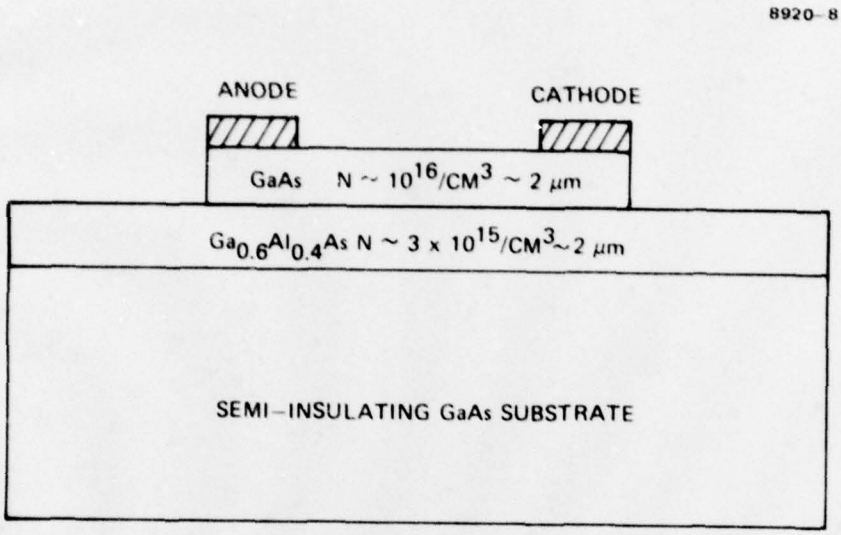

Figure 8. Cross section of a Gunn diode with optical waveguiding structure.

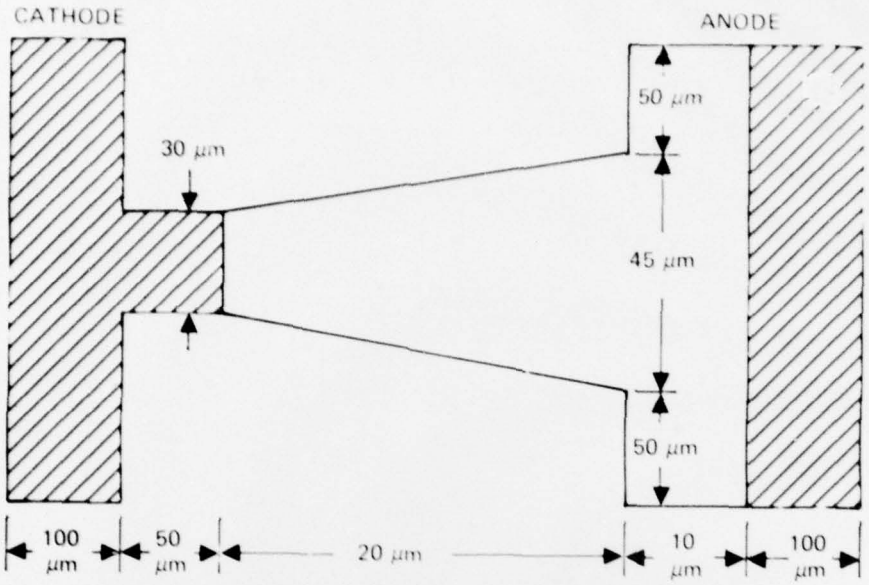

(a) Mask pattern.

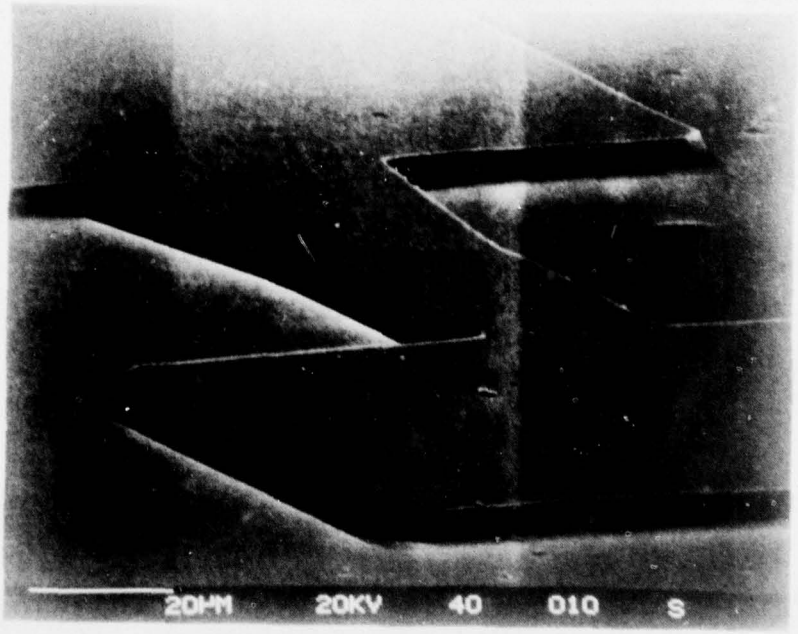

(b) Etched GaAs mesa.

Figure 9. Gunn diode active region pattern.

several Gunn diodes with lengths ranging from 20 to 100 μm. The diodes were tested using a curve tracer. Negative differential resistance was observed in all the diodes tested. Excellent uniformity of diode properties was obtained for diodes made from the same wafer. A typical I-V curve for a 20-μm diode is shown in Figure 10. We are currently testing the microwave properties of these diodes. An optical interaction study using these diodes will be carried out during the next quarter.

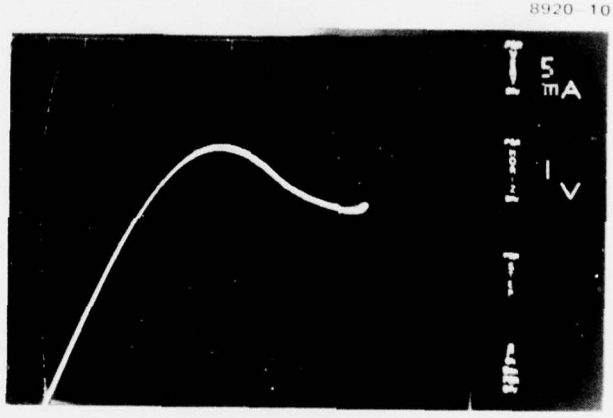

Figure 10. I-V curve of a 20-μm-long Gunn diode.

SECTION 5

PLANS FOR THE NEXT QUARTER

In the next quarter, we will finish the autocorrelation measurement setup so that the true pulse width of the output of the injection laser can be determined. We will attempt to modulate the laser at higher repetition frequencies and to improve the external cavity arrangment by such means as using an etalon in the cavity and adding an antireflection coating to the laser facet to keep the experimental parameters manageable. We will study the magnitude of the phase jitter in the optical pulse and find ways of reducing it.

We will continue the fabrication of GaAs FETs and Gunn diodes. RF characteristics of these devices will be measured so that appropriate microwave circuits can be designed for amplifier and oscillator operations. Optical-microwave interactions in these devices will then be studied quantitatively.

REFERENCES

1. M.G. Cohen, S. Knight and J.P. Elward, Appl. Phys. Lett. 8, 269 (1966).

2. P. Guetin and D. Boccon-Gibod, Appl. Phys. Lett. 13, 161 (1968).

3. P. Guetin, J. Appl. Phys. 40, 4114 (1969).

4. P.N. Butcher, W. Fawcett and C. Hilsum, J. Appl. Phys. 17, 841 (1966).

5. M. Nakamura, H. Kurona, T. Toyabe, M. Hirao and H. Kodera, Solid State Electron. 11, 583 (1968).